

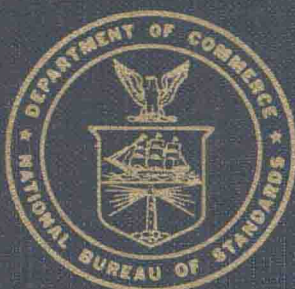
PHASE DIAGRAMS FOR CERAMISTS

VOLUME VIII

(Figures 7886–8180)

Bjorn O. Mysen

Compiled at the
NATIONAL INSTITUTE OF STANDARDS AND TECHNOLOGY
(formerly National Bureau of Standards)



Edited and Published by
THE AMERICAN CERAMIC SOCIETY, INC.

1990

Phase Diagrams for Ceramists

Volume VIII

General Editor

Bjorn O. Mysen
Geophysical Laboratory, Carnegie Institution of Washington

Associate Editor
Howard F. McMurdie, ACerS

Managing Editor
Helen M. Ondik, NIST

Editorial Associates
Mary A. Clevinger, NIST
Steven K. Peart, ACerS

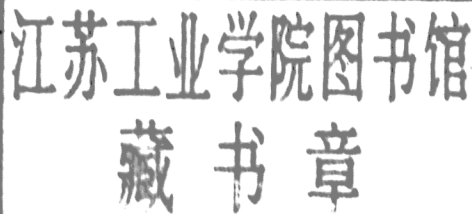
Graphics Systems
Peter K. Schenck, NIST

Text and Typesetting Systems
Carla G. Messina, ACerS

Compiled in the **Ceramics Division,**
National Institute of Standards and Technology
(formerly National Bureau of Standards)

The American Ceramic Society, Inc.

757 Brooksedge Plaza Drive, Westerville, Ohio 43081-2821





NSRDS

The National Standard Reference Data System comprises a set of data center and other data evaluation projects coordinated by the Standard Reference Data Program of the National Institute of Standards and Technology (NIST). The aim of this program is to provide reliable reference data on physical, chemical, and materials properties to the scientific and technical communities of the United States. Evaluated data produced under the program are made available in a variety of publications and computer-readable databases through joint projects of NIST and other interested groups, in this case the American Ceramic Society.

The Phase Diagrams published in this volume were collected and reviewed by the Phase Diagrams for Ceramists Data Center, located in the Institute for Materials Science and Engineering of the National Institute of Standards and Technology. Significant support from the American Ceramic Society was crucial in providing this important reference information to the ceramics community.

Malcolm W. Chase
Acting Director, Standard Reference Data
National Institute of Standards and Technology

ISBN 0-944904-23-8

No part of this book may be reproduced, stored in a retrieval system, or transmitted in any form or by any means, electronic, mechanical, photocopying, microfilming, recording, or otherwise, without written permission from the publisher.

Printed in the United States of America.

Copyright ©1990 by the U.S. Secretary of Commerce on behalf of the United States. This copyright is assigned to the American Ceramic Society

Preface

This volume is the eighth in the series *Phase Diagrams for Ceramists* and the third to appear since the National Institute of Standards and Technology (NIST) [formerly National Bureau of Standards] and the American Ceramic Society (ACerS) embarked on a jointly-sponsored Ceramic Phase Equilibria Program. The goal of the Program is to support growth and progress in the ceramics industry by providing relevant critically-evaluated phase diagrams. To achieve this, a multiyear program was established to improve currency with the archival literature and to provide critically-evaluated phase diagrams for oxides, salts, carbides, nitrides, borides, compound semiconductors, and chalcogenides. Computer graphics, database management, computer evaluation and predictive modeling are being used where possible to produce databases for distribution and generation of computer-typeset products. Program updates appear periodically in the American Ceramic Society Bulletin.

Program Origins: For over fifty years the National Bureau of Standards (now NIST) and ACerS have collaborated on the publication of evaluated phase diagrams of ceramic systems, best represented by the series *Phase Diagrams for Ceramists*, Volumes I-V. The joint Ceramic Phase Equilibria Program, representing a continuation and

expansion of the effort to make ceramic phase information readily and comprehensively available, was initiated in December 1982.

Program Responsibility: To achieve the goals of the expanded program a multiyear effort was established with support from NIST and other federal agency programs and from a fund-raising effort managed by the ACerS. NIST provides overall coordination and technical guidance and ensures quality data coverage and evaluation. NIST has also developed a prototype PC graphics database. The ACerS is responsible for the production aspects and dissemination of the data in both printed and computer database forms.

Sponsorship: The fund-raising effort managed by ACerS is an ongoing activity. As of June 1989 a total of \$2,486,410 has been contributed or pledged to the program. There are five basic categories of participation in the Ceramic Phase Equilibria Program: Primary Sponsors, \$200,000 or more; Sponsors, \$100,000 or more; Affiliate Sponsors, \$25,000 or more; Contributors, \$5,000 or more; and Members and Friends, any smaller amount. Contributions to the program, through June 1989, from individuals and the following organizations are gratefully acknowledged.

PRIMARY SPONSORS

Corning Glass Works
IBM Corporation
Matsushita Electrical Industrial Co., Ltd. (Japan)
The American Ceramic Society, Inc.

PRIMARY SPONSORS-FEDERAL

Ceramics Division, NIST
Defense Advanced Research Projects Agency
Standard Reference Data, NIST

SPONSORS

Allied-Signal Corp.
Aluminum Co. of America
Battelle Memorial Institute
Norton Co.
Owens-Corning Fiberglass Corp.

AFFILIATE SPONSORS

Asahi Glass Co., Ltd.
Asahi Glass Foundation for Industrial Technology (Japan)
AT&T Bell Labs
B & B Refractories, Inc.
Buehler Ltd.
Cabot Corp. Foundation
Coors Ceramic Co.
E. I. du Pont de Nemours & Co., Inc.
Ford Motor Co.
General Motors Corporation
GTE Labs, Inc.
Hitachi Ltd. (Japan)
Kyocera Corporation
Murata Mfg. Co., Ltd. (Japan)
NGK Insulators, Ltd.
NGK Spark Plug Co., Ltd.
PPG Industries
Rhône-Poulenc, Inc.
3M Co. Foundation

AFFILIATE SPONSORS-FEDERAL

Department of Energy*
National Science Foundation*

CONTRIBUTORS

Alcan International, Ltd.
Alfred University
Foundation for Promotion of Materials Science and
Technology in Japan
Harbison-Walker Refractories, Co., Div. of Dresser Industries
Hitachi Chemical Co., Ltd. (Japan)
Hitachi Metals Ltd. (Japan)
Owens-Illinois, Inc.
Serbian Academy of Sciences and Arts
Shell Development Co.
Richard M. Spriggs
William H. Payne

SECTIONS, MEMBERS, AND MATCHING GIFTS

10 ACerS Sections
11 Distinguished Life Members and Past Presidents
584 Individual Members
30 Industrial Matching Gifts

* Through the Joint Program on Critical Compilation of Physical and Chemical Data coordinated by Standard Reference Data at NIST.

INTRODUCTION

This volume, VIII, in the *Phase Diagrams for Ceramists* series includes 295 Figures containing 915 diagrams of systems collected from the literature between 1975 and 1983,¹ together with some overflow from earlier volumes.

The systems include oxide and salt systems with and without water, most at pressures above ambient atmospheric pressure. The following diagrams are at atmospheric pressure: 7887A, 7889, 7894A, 7897, 7898, 7900, 7904, 7917, 7919, 7920, 7931, 7948, 7952, 7958, 8126, 8127, 8134, 8135, 8136A, 8136B, 8146, 8147, and 8149.

A significant portion of the diagrams, in particular those from chemically complex systems, is from the earth science literature. Those diagrams, and diagrams obtained at pressures above ambient, are particularly relevant to earth science. Water and other volatile components (CO_2 , CH_4 , N_2) are of central interest and their influence on phase relations, particularly in alkali metal - alkaline earth - alumina - silica systems at high pressure (above ambient), is a principal focus among earth scientists using and generating phase diagrams. Diagrams for such systems were included because of their general relevance and because this expansion makes *Phase Diagrams for Ceramists* more attractive to a wider audience of phase diagram users.

Those diagrams and others in this compilation not only will aid a wide audience of phase diagram users, but also illustrate that the *Phase Diagrams for Ceramists* series is intended for all materials scientists, including those studying earth materials. The chemical compositions and physical conditions often vary from discipline to discipline, but the practical and principal use of phase diagrams is the same. Phase diagrams relevant to a particular problem may be published in literature not readily available or not viewed as relevant. The compilation in Volume VIII should assist in making the literature accessible to all users of phase diagrams.

The reader should note that the indexes in this volume are cumulative for Volumes VI, VII, and VIII. Cumulative indexes for Volumes I, II, and III were published in Volume III and a separate volume of indexes was published in 1984 covering Volumes I through V.

Individuals whose names do not appear on the title page who deserve acknowledgement and thanks for their contributions to the publication of this book are acknowledged here.

The software used for generating and editing the database and the commentaries, and for computer typesetting, is the series of programs written by Carla G. Messina. Thanks also go to Kimberly M. Kessell for assistance in running the computer-typesetting programs.

The graphics programs with which diagrams were digitized, edited, and plotted are those used for Volumes VI and VII, written by

Peter K. Schenck with Jennifer R. Dennis Verkouteren. The following persons assisted in the phase diagram graphics data effort to produce Volume VIII: Michael Rodtang, Daniel Pennington, Raymond Yang, Thomas Green, Theresa Messina, and Barbara Lee.

For a fuller discussion of the procedures used in collecting, evaluating, and editing the diagram information, and a description of the computer graphics software used in digitizing, storing, retrieving, and plotting the phase diagrams, the reader is referred to the "General Guidelines" and "Graphics Program" sections in Volume VI.

The individuals listed below are the editors who contributed to Volume VIII. The commentaries submitted by each are identified in the book by the initials shown.

M.F.B.	Michael F. Berard, Iowa State University, Ames
L.L.Y.C.	Luke L. Y. Chang, University of Maryland, College Park
L.P.C.	Lawrence P. Cook, National Institute of Standards and Technology
F.P.G.	Fredrik P. Glasser, University of Aberdeen, Old Aberdeen, Scotland
D.K.	Drago Kolar, Institut "Josef Stefan," Yugoslavia
C.M.K.	Carolyn M. Kramer, The Gillette Company, Cambridge, Massachusetts
E.R.K.	Eric R. Kreidler, Ohio State University, Columbus
C.K.K.	C. K. Kuo, Shanghai Institute of Ceramics, Chinese Academy of Sciences
R.W.L.	Robert L. Luth, Geophysical Laboratory, Carnegie Institution of Washington
B.O.M.	Bjorn O. Mysen, Geophysical Laboratory, Carnegie Institution of Washington
T.J.R.	Thomas J. Rockett, University of Rhode Island, Kingston
R.S.R.	Robert S. Roth, National Institute of Standards and Technology
C.E.S.	Charles E. Semler, Ohio State University, Columbus
S.S.	Shigeyuki Somiya, Nishi-Tokyo University, Japan
J.W.	Johannes Weiss, Renker GmbH, Freiburg, West Germany
D.R.W.	David R. Wilder, Iowa State University, Ames

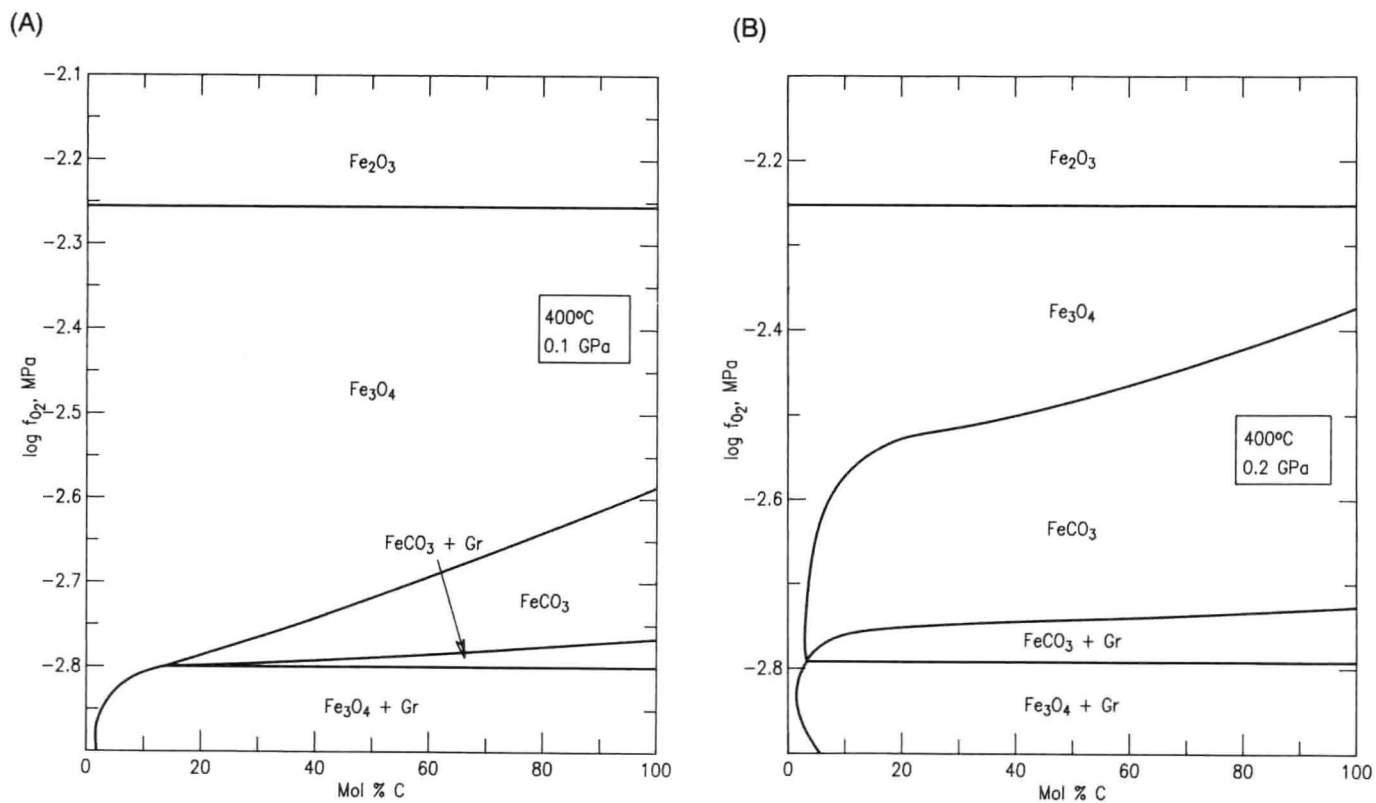
1. C. G. Messina, M.A. Clevinger, L. P. Cook, and R.S. Roth, *Phase Diagrams for Ceramists Bibliographic Update for Oxides and Salts through January 1, 1984*, 182 pp (The American Ceramic Society, Inc., Westerville, Ohio, January 1986).

TABLE OF CONTENTS*

	Page
Preface	v
Introduction	vii
A. Oxygen Plus Iron Plus Carbon Plus Hydrogen.....	1
B. Oxides Only	4
I. Two Oxides	4
II. Three Oxides	6
III. Four Oxides	7
IV. Five Oxides	16
V. Six Oxides	23
C. Oxides Plus Water	24
I. One Oxide Plus Water	24
II. Two Oxides Plus Water	36
III. Three Oxides Plus Water	66
IV. Four Oxides Plus Water	113
V. Five Oxides Plus Water	147
VI. Six Oxides Plus Water	164
VII. Seven Oxides Plus Water	171
VIII. Eight Oxides Plus Water	175
IX. Nine Oxides Plus Water	176
D. Oxides Plus Water Plus Oxyanion Salts	187
I. One Oxide Plus Water Plus One Oxyanion Salt	187
II. Two Oxides Plus Water Plus One Oxyanion Salt	188
III. Three Oxides Plus Water Plus One Oxyanion Salt	189
IV. Four Oxides Plus Water Plus One Oxyanion Salt	191
E. Oxides Plus Water Plus One Oxyanion Salt and One Halide	193
F. Oxides Plus Water Plus Halides	196
I. One Oxide Plus Water Plus One Halide	196
II. Two Oxides Plus Water Plus One or Two Halides	199
III. Three Oxides Plus Water Plus One Halide	203
IV. Four Oxides Plus Water Plus One or Two Halides	209
V. Five Oxides Plus Water Plus One or Three Halides	214
G. Oxides Plus Water Plus One Halide Plus One Gas	220
H. Oxides Plus Water Plus Others	224
I. One Oxide Plus One Nitrate Plus One Gas	224
II. Two Oxides Plus Water Plus One Metal Plus Sulfur	226
III. Three Oxides Plus Water Plus Carbon Plus Two Gases	230

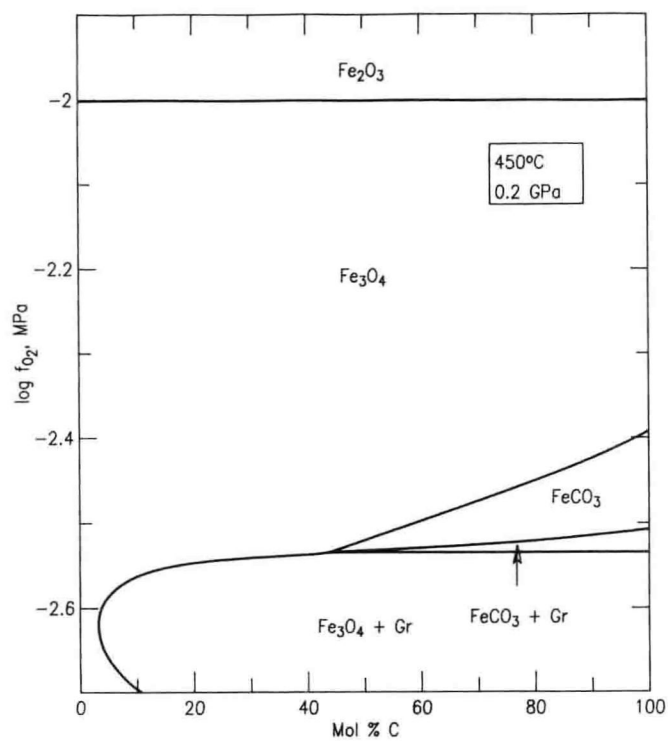
*Except for certain Figures as noted in the Introduction, all of the systems included in this volume were studied at pressures above ambient atmospheric pressure.

I. Oxides Plus Water Plus Gases	232
I. One Oxide Plus Water Plus One Gas	232
II. Two Oxides Plus Water Plus One Gas	237
III. Three Oxides Plus Water Plus One Gas	248
IV. Three Oxides Plus Water Plus Two Gases	268
V. Four Oxides Plus Water Plus One Gas	269
VI. Five Oxides Plus Water Plus One Gas	271
VII. Five Oxides Plus Water Plus Two Gases	273
VIII. Six Oxides Plus Water Plus One Gas	275
IX. Nine Oxides Plus Water Plus One Gas	279
J. Oxides Plus Others	281
I. Three Oxides Plus One Oxyanion Salt	281
II. Three Oxides Plus Sulfur	283
K. Oxides Plus Gases	285
I. Two Oxides Plus One Gas	285
II. Two Oxides Plus Three Gases	292
III. Three Oxides Plus One Gas	296
IV. Four Oxides Plus One Gas	308
V. Nine Oxides Plus One Gas	310
L. Water Only	313
M. Water Plus Others	314
I. Water Plus Oxyanion Salts or Acids	314
a. Water Plus One Oxyanion Salt or Acid	314
b. Water Plus One Oxyanion Salt and One Acid	318
II. Water Plus Halogen or Halide	318
a. Water Plus Bromine or One Bromide	318
b. Water Plus One Chloride	322
c. Water Plus One Iodide	326
III. Water Plus Two Acids	327
IV. Water Plus Two Metals Plus Sulfur	328
V. Water Plus One Salt Plus One Gas	330
N. Water Plus Gases	335
I. Water Plus One Gas	335
II. Water Plus Two Gases	355
O. Carbon Plus Hydrogen Plus Oxygen	357
Errata	363
Author Index	365
System Index	375

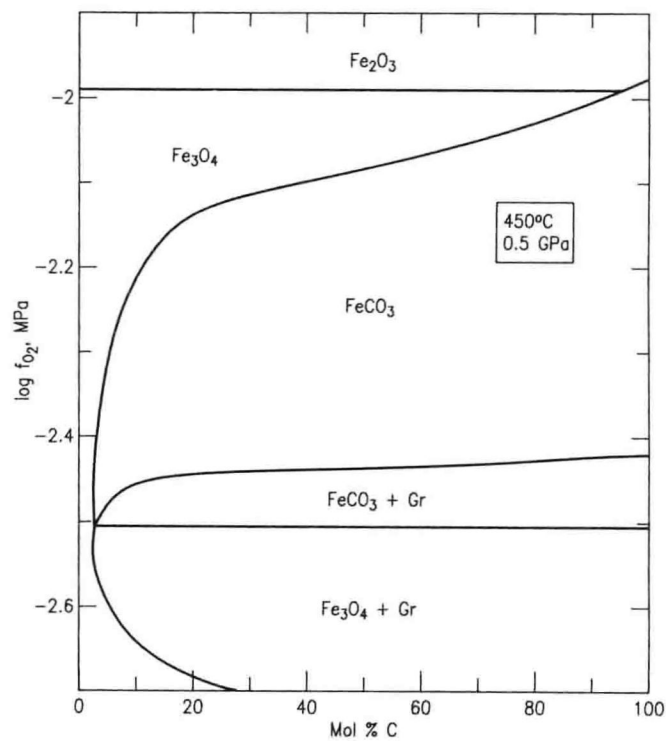
A. OXYGEN PLUS IRON PLUS CARBON PLUS HYDROGEN**O-Fe-C-H₂**

O-Fe-C-H₂ (cont.)

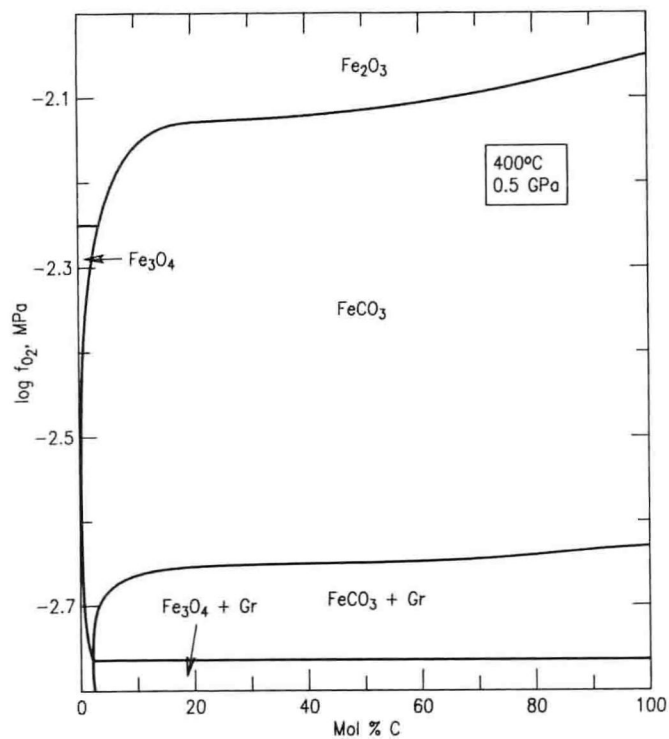
(C)



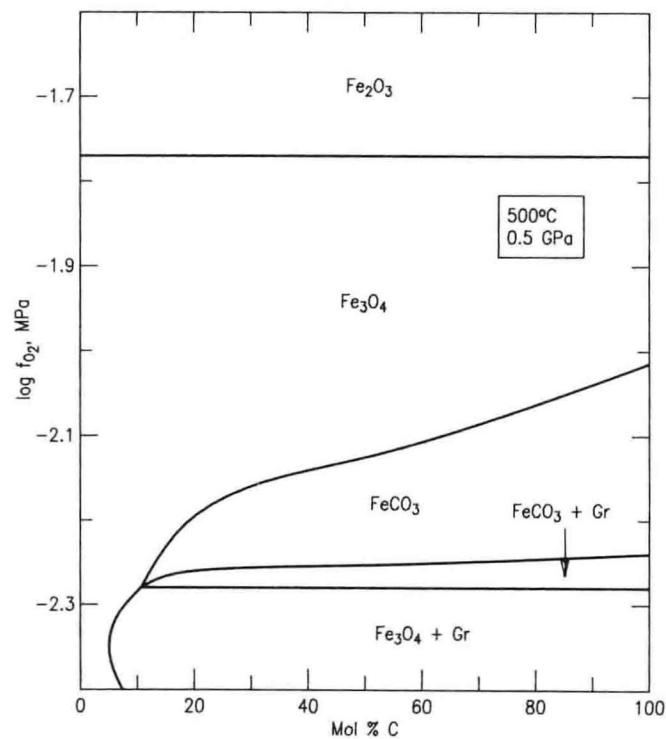
(E)



(D)



(F)



O-Fe-C-H₂ (concl.)

(G)

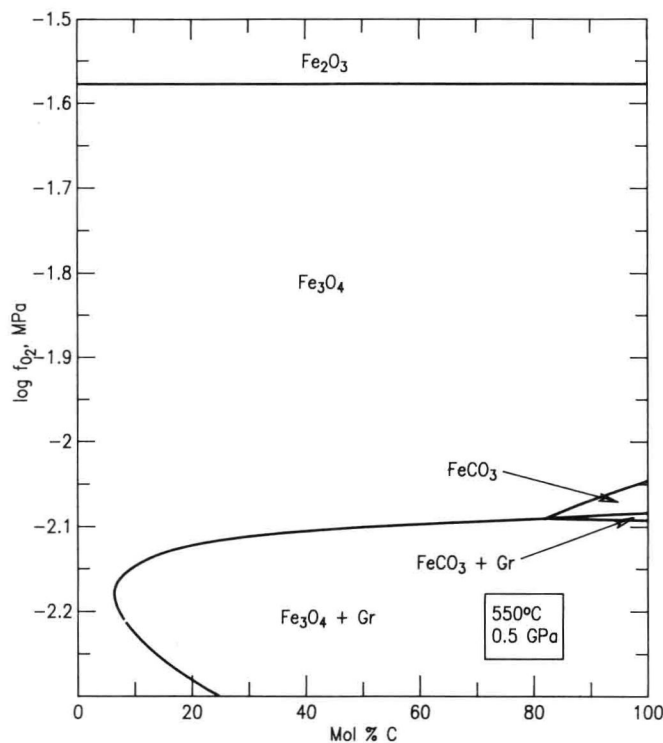
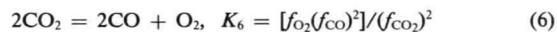
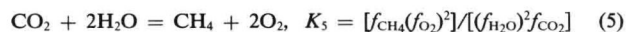
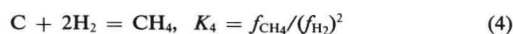
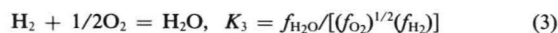
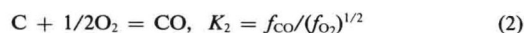


Fig. 7886—System FeO-Fe₂O₃-FeCO₃-C. (A-G) log f_{O_2} vs mol% C as a function of temperature and pressure. Gr = graphite.
B. R. Frost, *Am. J. Sci.*, **279** [9] 1033-1059 (1979).

The stability of graphite in the presence of a C-O-H fluid has been calculated at pressures up to 1.0 GPa at temperatures above 400°C. In fluids not in equilibrium with graphite, fluid compositions have been calculated as a function of oxygen fugacity (f_{O_2}) at constant pressure and temperature. The system contains the species H₂O, CO₂, O₂, H₂, CO, and CH₄. The equilibrium constants used in the calculations, for the following reactions, are from the JANAF Tables.¹

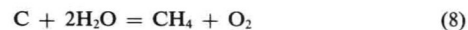


The standard states for the fluids are 0.1 MPa at any specified temperature and for the solids, any specified pressure and temperature. Fugacity coefficients of the fluids were determined from the expressions of Ref. 2 as modified by Refs. 3 and 4. For pure fluids, the calculated fugacity coefficients are within $\pm 10\%$ of measured values. Adjustments have been made for CO₂ + H₂O fluids to fit experimentally determined fugacity coefficients.⁴ Relevant thermodynamic data are tabulated. For more complex fluids, no experimental data are available to check the accuracy of the calculated fugacity coefficients. In addition, the relationship given in Eq. 7 and the carbon content of the gas, X_C , are fixed.

$$P_{\text{fluid}} = P_{H_2O} + P_{CO_2} + P_{H_2} + P_{CO} \quad (7)$$

The X_C is the molar ratio of carbon to hydrogen in the system.

At low f_{O_2} , the equilibria in Eqs. 3 and 4 govern the equilibria shown in Eq. 8 and the carbon content of the fluid decreases with increasing oxygen fugacity.



The $X_{H_2O}^{max}$ is the maximum H₂O content for a fluid in equilibrium with graphite. This value increases rapidly with increasing pressure because the activity coefficient of CO₂ increases very rapidly with pressure,⁵ whereas that of H₂O is nearly constant.

Relationships between redox equilibria of iron-bearing minerals and fluid compositions have been shown in the system Fe-C-O-H (A-G) as a function of X_C and f_{O_2} at a range of pressures and temperatures. Note in particular the extension of the siderite (FeCO₃) stability field to increasingly water-rich fluid compositions with increasing pressures.

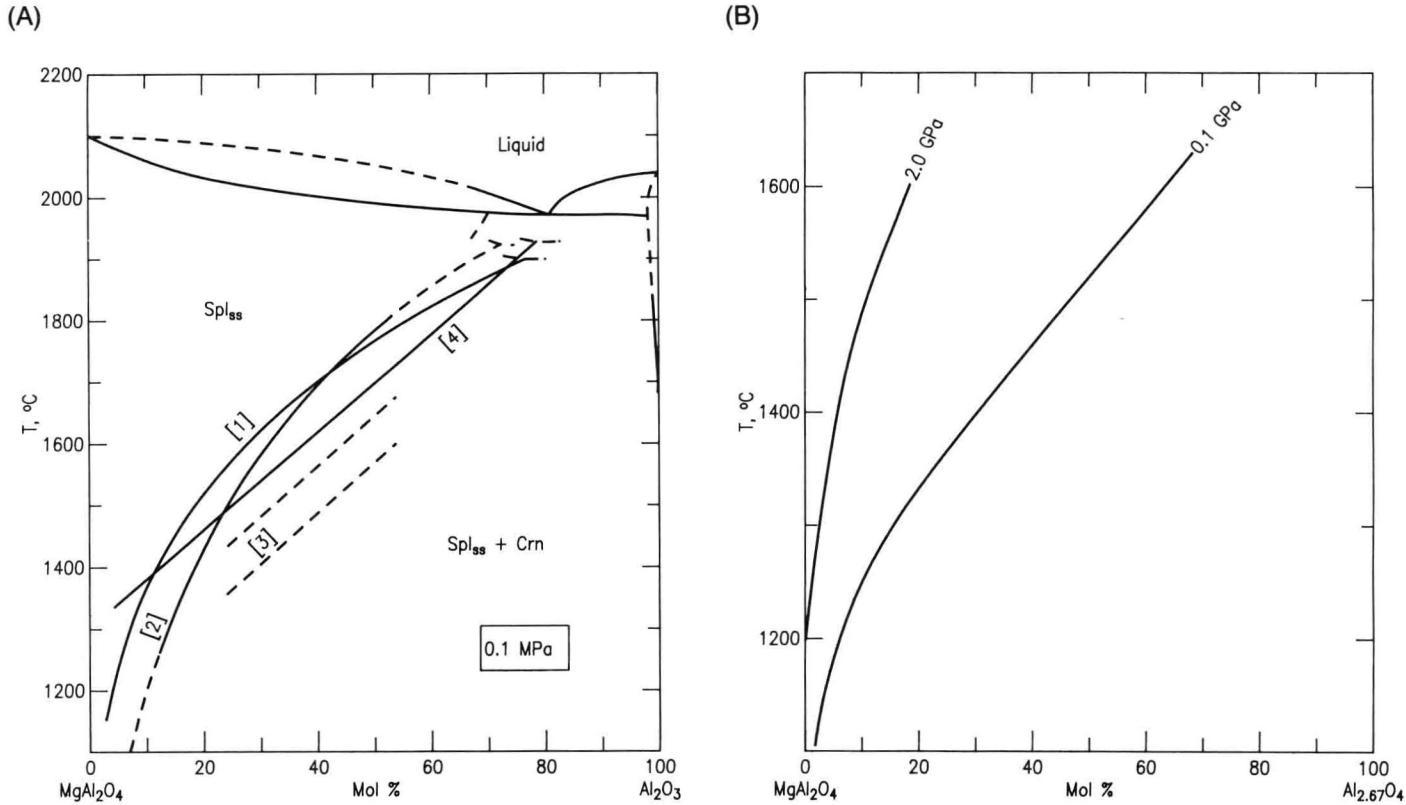
The results have been applied to discussion of metamorphism in the crust of the earth.

1. D. R. Stull and H. Prophet, JANAF Thermochemical Tables, 2nd Ed., NSRDS-NBS-31, 1141 pp. U. S. Dept. of Commerce, Washington, D.C. 1971.
2. O. Redlich and J. N. S. Kwong, *Chem. Rev.*, **44**, 233 (1949).
3. R. deSantis, G. J. F. Breedveld, and J. M. Prausnitz, *Ind. Eng. Chem. Process. Des. Dev.*, **13** [4] 374 (1974).
4. J. R. Holloway, pp. 161-181 in *Thermodynamics in Geology*. Edited by D. G. Fraser. Boston, 1977.
5. G. B. Skippen, pp. 66-83 in *Mineralogical Association of Canada Short Course in Application of Thermodynamics to Petrology and Ore Deposits*. Edited by H. J. Greenwood. Mineralog. Assoc. Canada, Vancouver, 1977.

B.O.M.

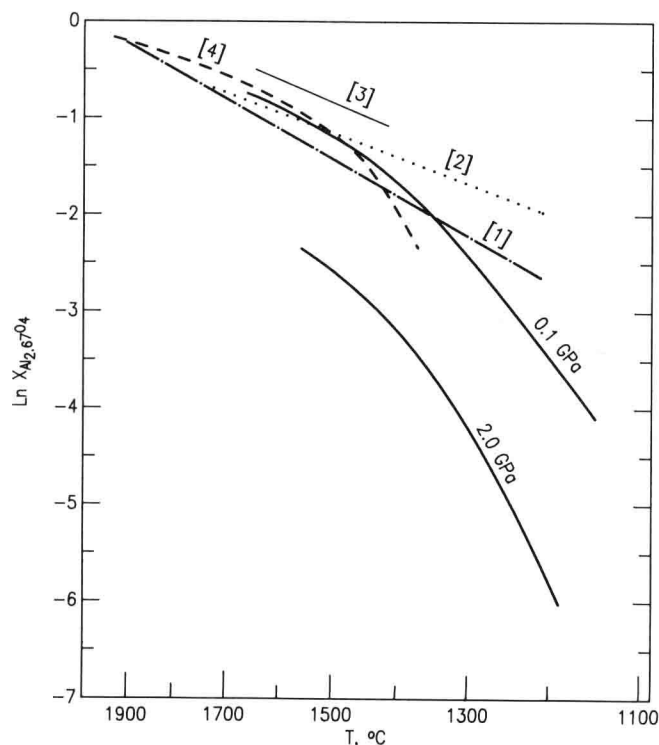
B. OXIDES ONLY
I. Two Oxides

MgO-Al₂O₃



MgO-Al₂O₃ (concl.)

(C)



(D)

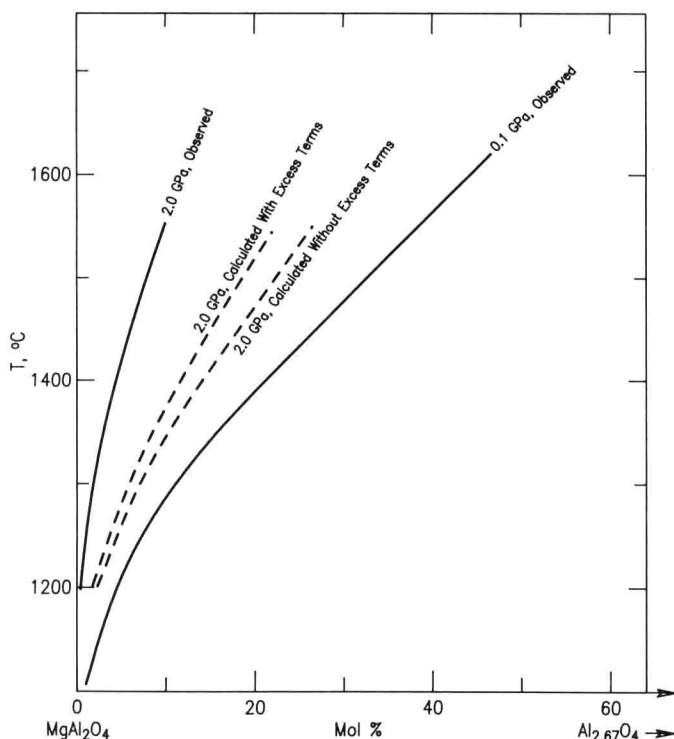


Fig. 7887—System $\text{MgAl}_2\text{O}_4\text{-Al}_2\text{O}_3$. (A) Phase relations at 0.1 MPa (data from Refs. 1-4); (B) experimental results on defect spinel solid solution with Al_2O_3 at 0.1 and 2.0 GPa; (C) temperature-composition relations on the join $\text{MgAl}_2\text{O}_4\text{-Al}_{2.67}\text{O}_4$; (D) comparison of experimental results on defect spinel Al_2O_3 solid solubility and behavior predicted by models with and without consideration of excess mixing properties. Spl_{ss} = spinel solid solution (MgAl_2O_4); Crn = corundum (Al_2O_3). Numbers on lines refer to references.

H. U. Viertel and F. Seifert, *Neues Jahrb. Mineral., Abh.*, **140** [1] 89-101 (1980).

Stability relations were studied at 0.1 GPa (internally heated, gas-media apparatus) and at 2.0 GPa (solid-media, high-pressure apparatus) with mixtures of defect spinel¹ and Al_2O_3 as starting materials. A summary of previous data on this join, obtained at 0.1 MPa pressure, is shown in (A). The temperatures were measured with Pt-Pt90Rh10 thermocouples. Although no calibration methods are reported, the temperature uncertainties are reported as $\pm 10^\circ$ and $\pm 20^\circ\text{C}$, respectively, at 1200° and 1600°C in the gas-media, high-pressure apparatus and as $\pm 25^\circ\text{C}$ at all temperatures in the solid-media, high-pressure apparatus. Pressure uncertainties (no calibration reported) are given as ± 5.0 MPa and ± 0.1 GPa in the gas-media, and solid-media, high-pressure apparatus, respectively. Experimental charges were examined by X-ray diffraction (with Si as internal standard), using the calibration methods of Ref. 5 to determine the spinel compositions.

Experimental results at 0.1 and 2.0 GPa (B) show that the solubility of Al_2O_3 increases isothermally with decreasing pressure and isobarically with increasing temperature. It is clear, however, from the representation in (C) that the solution cannot be considered ideal. The pressure effect is most likely due to the significant molar volume difference (12%) between ideal hercynite and defect spinel.⁵ Modeling of the solubility behavior was also attempted using a regular solution model, but with no consideration of ΔV being pressure dependent (D). Although inclusion of an excess mixing term improves the calculated results, the model does not approach the experimental values. Most likely, this lack of agreement is due to ignoring the pressure dependence of the ΔV , as the molar volume of the defect spinel is pressure dependent.

1. A. M. Lejus and R. Collongues, *Bull. Soc. Chim. Fr.*, **1961**, 65 (1961).
2. D. M. Roy, R. Roy, and E. F. Osborn, *Am. J. Sci.*, **251** [5] 337 (1953).
3. H. Saalfeld and H. Jagodzinski, *Z. Kristallogr.*, **109** [2] 87 (1957).
4. K. Shirasuka and G. Yamaguchi, *Yogyo Kyokashishi*, **82** [12] 650 (1974).
5. H. U. Viertel and F. A. Seifert, *Neues Jahrb. Mineral. Abh.*, **134** [2] 167 (1979).

B.O.M.

II. Three Oxides

NiO-Al₂O₃-SiO₂

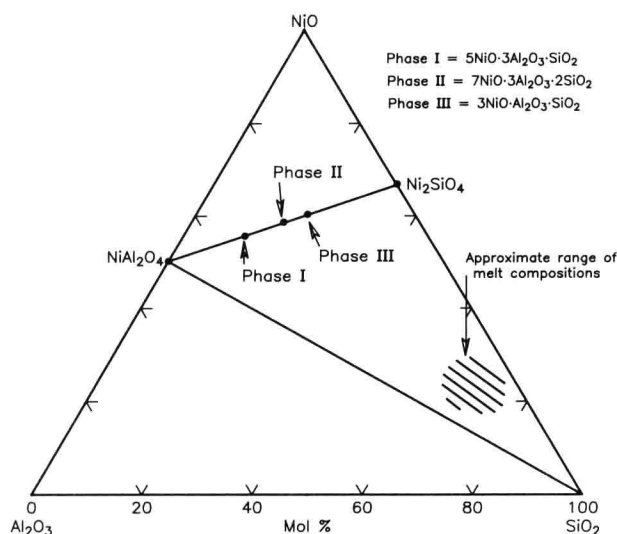


Fig. 7888—System NiO-Al₂O₃-SiO₂. Composition triangle depicting location of three new phases (see text) and approximate composition of coexisting melt.

C. B. Ma, *Neues Jahrb. Mineral., Monatsh.*, No. 3-4, 113-126 (1974).

Solid-media, high-pressure apparatus¹ and Pt-wound vertical quench furnaces were used for the experiments. Temperatures were measured with Pt-Pt87Rh13 thermocouples. In these experiments, $\pm 10^\circ\text{C}$ and $\pm 10\%$ uncertainties in temperature and pressure, respectively, were reported.² Starting materials were analytical grade Al(OH)₃, NiCO₃, and H₄SiO₄, sintered at 1400°C before use. These materials were loaded in crimped, but not sealed, Pt and Ag capsules. Optical, X-ray and electron microprobe methods were employed for sample identification and analysis.

Three new phases, grown in equilibrium with the melt, are reported. Their detailed crystallographic and chemical compositions are reported. Ideally formulated, these phases are I, Ni₅Al₆SiO₁₆, II, Ni₇Al₆Si₂O₂₀, and III, Ni₃Al₂SiO₈. These orthorhombic crystalline phases may be portions of a homologous series of the type M_{2n}O_{n-1}T_nO_{3n+1} with M and T being octahedrally and tetrahedrally coordinated cations, respectively.³

1. F. R. Boyd and J. L. England, *JGR, J. Geophys. Res.*, **65** [2] 741 (1960).
2. C. B. Ma, Ph.D. Thesis, Harvard University, 1972.
3. P. B. Moore and J. V. Smith, *Phys. Earth Planet. Int.*, **3**, 166 (1970).

B.O.M.

III. Four Oxides

K_2O - FeO - Al_2O_3 - SiO_2

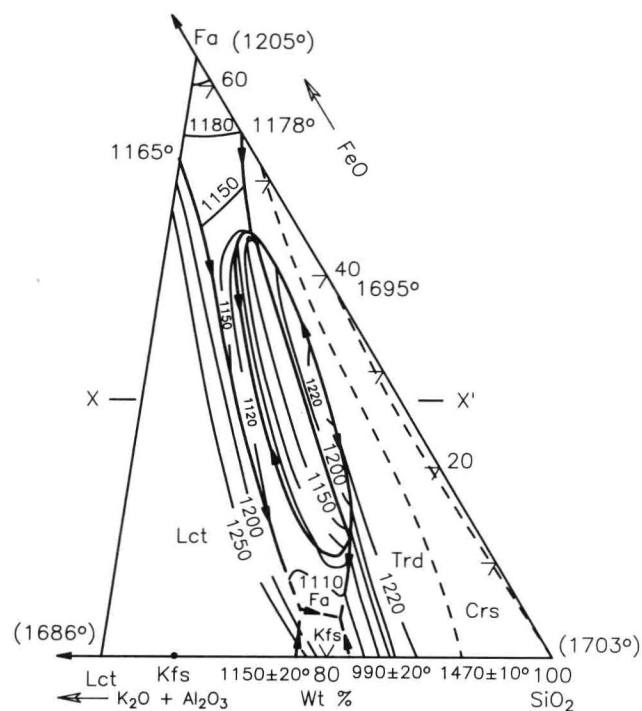


Fig. 7889—System Fe_2SiO_4 - $KAlSi_2O_6$ - SiO_2 . Liquidus relations. Trd = tridymite (SiO_2); Crs = cristobalite (SiO_2); Fa = fayalite (Fe_2SiO_4); Kfs = K-feldspar ($KAlSi_3O_8$); Lct = leucite ($KAlSi_2O_6$).

W. Visser and A. F. Koster van Groos, *Am. J. Sci.*, **279** [8] 970-988 (1979).

W. Visser and A. F. Koster van Groos, *Am. J. Sci.*, **279** [10] 1160-1175 (1979).

Starting materials for experiments in Mo-heated, vertical 0.1 MPa quench furnaces were leucite gel, SiO_2 , Fe_2O_3 , and Fe metal powder. The experiments were conducted with controlled oxygen fugacity (f_{O_2}) between that of the Fe-FeO and Mo-MoO₂ oxygen buffers. Temperature measurement and control were not discussed. Experimental charges were examined with optical microscopy and with the electron microprobe. No iron-loss, but up to 17% K-loss (relative), was reported.

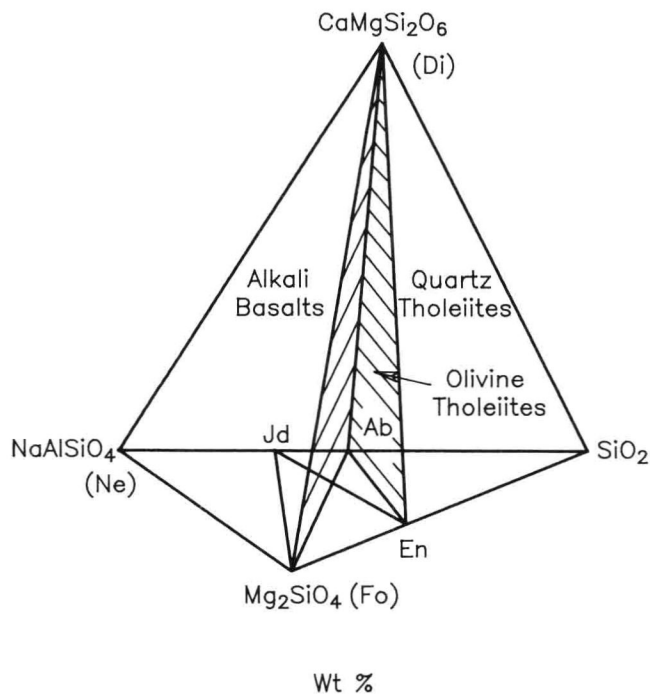
The diagram shows the liquid-liquid phase relations revised after that of Fig. 801, and represents the information reported by Ref. 1. The original source does not discuss why a revision of the original phase diagram was necessary, but it probably results from suggested problems with Fe- and K-loss in the original experiments. In that case, this diagram should be used, since it is the result of more carefully executed and monitored experiments.

1. W. Visser and A. F. Koster van Groos, *Trans., Am. Geophys. Union*, **59** [4] 401 (1978).

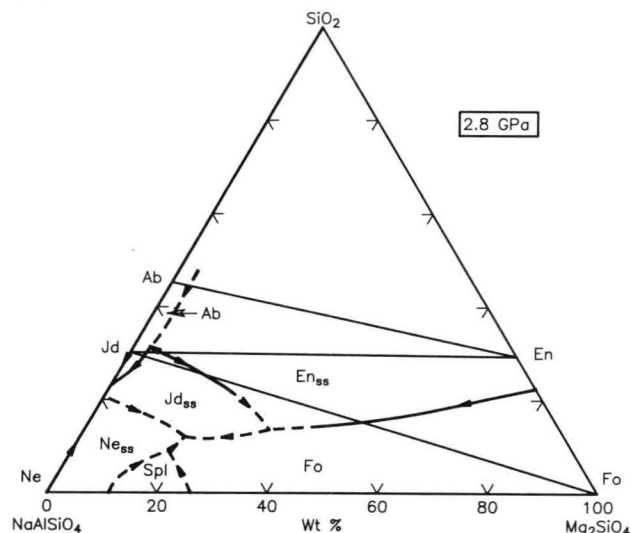
B.O.M.

Na_2O - MgO - Al_2O_3 - SiO_2

(A)

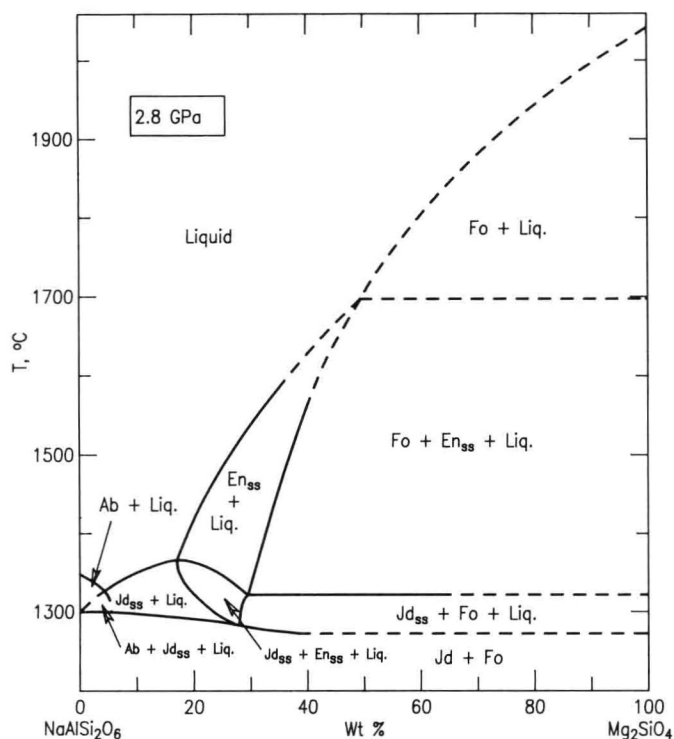


(B)

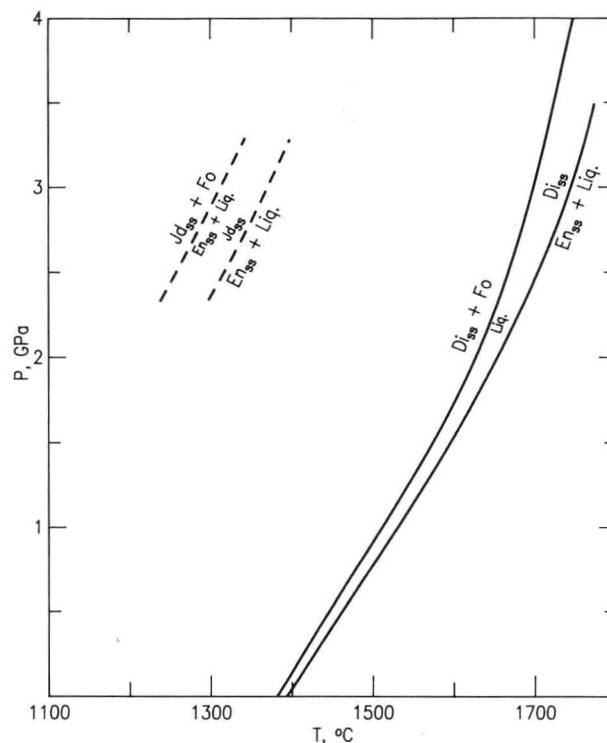


Na₂O-MgO-Al₂O₃-SiO₂ (cont.)

(C)



(E)



(D)

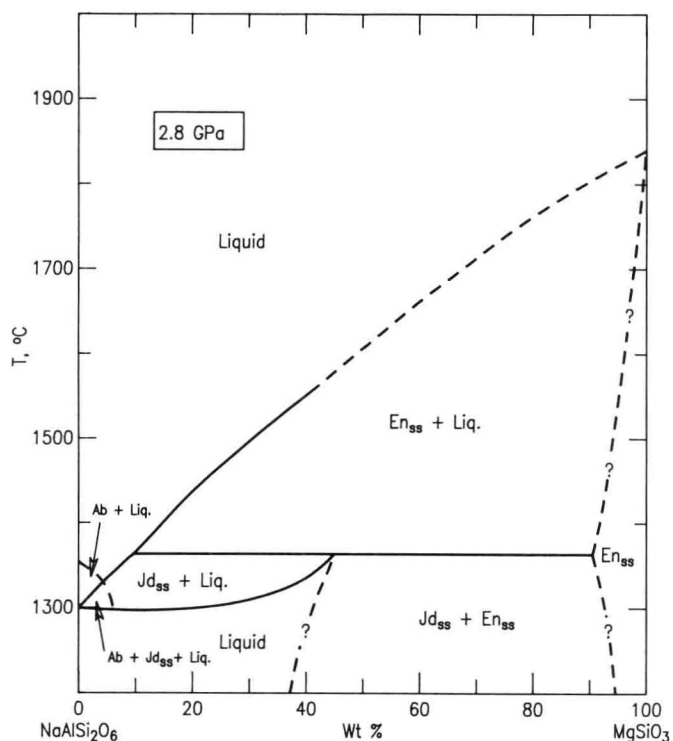


Fig. 7890—System Na₂O-MgO-Al₂O₃-SiO₂. (A) Location of the jadeite-forsterite and jadeite-enstatite joins relative to other petrologically relevant joins and planes in the basalt tetrahedron (Ref. 1); (B) liquidus diagram for the subsystem NaAlSiO₄-Mg₂SiO₄-SiO₂ at 2.8 GPa (data from Refs. 2 and 3); (C) temperature-composition section (at 2.8 GPa) for the join NaAlSi₂O₆-Mg₂SiO₄; (D) temperature-composition section (at 2.8 GPa) for the join NaAlSi₂O₆-MgSiO₃; (E) comparison of the pressure-dependence of the solidus temperatures of jadeite + enstatite and jadeite + forsterite with diopside + enstatite and diopside + forsterite (Ref. 4). Di = diopside (CaMgSi₂O₆); Fo = forsterite (Mg₂SiO₄); En = enstatite (MgSiO₃); Ne = nepheline (NaAlSi₃O₈); Ab = albite (NaAlSi₃O₈); Jd = jadeite (NaAlSi₂O₆); Spl = spinel (MgAl₂O₄); Liq = liquid; ss = solid solution.

K. E. Windom and A. L. Boettcher, *Am. J. Sci.*, **281** [3] 335-351 (1981).

Starting materials were synthetic forsterite and enstatite prepared with the gel method described by Ref. 5 and natural jadeite from New Idria, California.⁶ The starting materials were contained in sealed Pt containers and subjected to pressure and temperature in the solid-media, high-pressure apparatus with Pt-Pt90Rh10 thermocouples for temperature measurement. Calibration methods for pressure and temperature are reported by Ref. 7 and given as $\pm 5\%$ and $\pm 10^\circ\text{C}$, respectively. Experimental durations ranged from 0.5 to 8 h, and the experimental conditions were reversed. Experimental charges were examined with optical microscopy and with X-ray powder diffraction.

The liquidus phase relations in the system Mg₂SiO₄-NaAlSiO₄-SiO₂ characteristically exhibit a large enstatite liquidus field at 2.8 GPa. On the join enstatite-jadeite, the principal topological features resemble those for the join enstatite-diopside,⁴ but the melting temperatures are about 400°C lower. This temperature difference presumably at

Na₂O-MgO-Al₂O₃-SiO₂ (concl.)

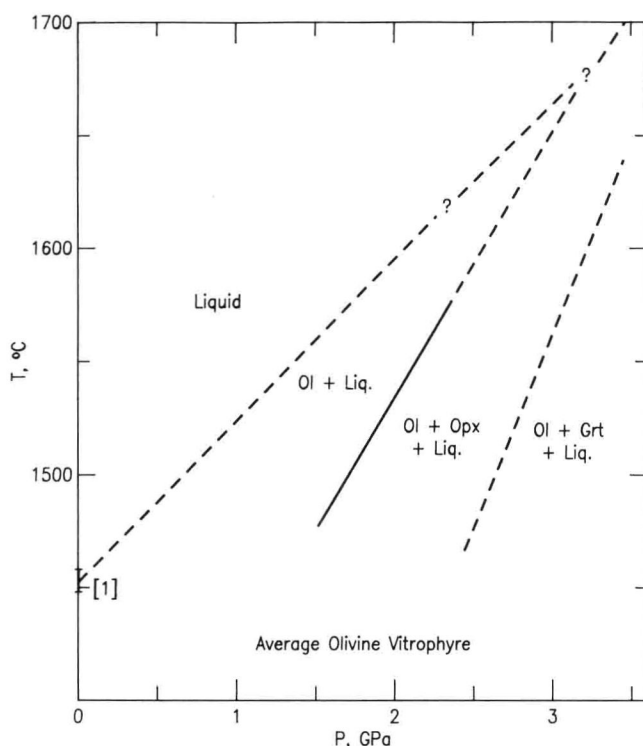
least partly is controlled by extensive solubility of the MgSiO₃ component in jadeite. The liquidus phase relations on the join forsterite-jadeite exhibit few similarities to the analogous join, forsterite-diopside.⁴ Whereas, in the forsterite-jadeite join, forsterite, enstatite, jadeite, and albite are liquidus phases, only forsterite and diopside occur on the liquidus on the forsterite-diopside join.

1. H. S. Yoder, Jr. and C. E. Tilley, *J. Petrol.*, **3**, 342 (1962).
2. P. M. Bell and E. H. Roseboom, Jr., *Mineral. Soc. Am. Spec. Pap.*, **2**, 151 (1969).
3. C. H. Chen and D. C. Presnall, *Am. Mineral.*, **60** [5-6] 398 (1975).
4. I. Kushiro, *Am. J. Sci.*, **267A**, 269-294 (1969).
5. W. C. Luth and C. O. Ingamells, *Am. Mineral.*, **50** [1-2] 255 (1965).
6. R. G. Coleman, *J. Petrol.*, **2**, 209 (1961).
7. K. E. Windom and A. L. Boettcher, *Am. Mineral.*, **61** [9-10] 889 (1976).

B.O.M.

CaO-FeO-MgO-SiO₂

(A)



(B)

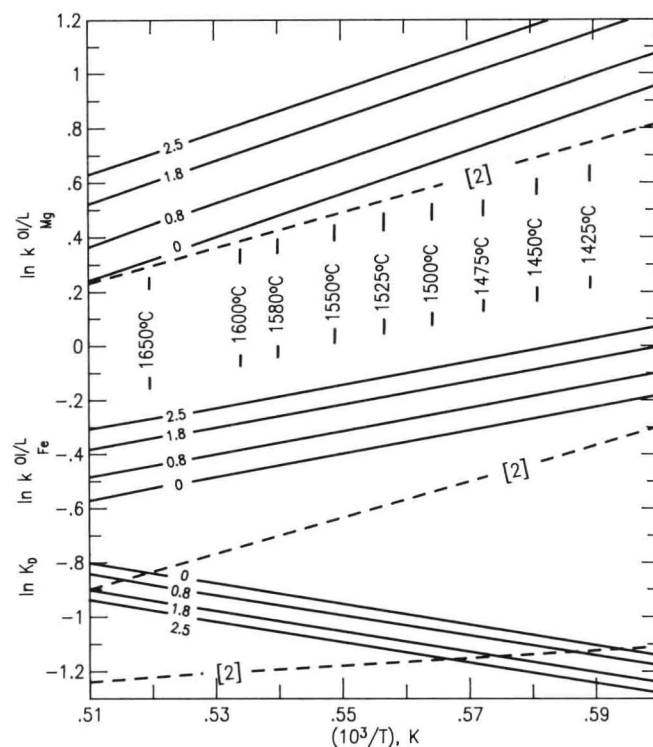


Fig. 7891—System CaO-FeO-MgO-SiO₂. (A) Pressure-temperature stability relations of average lunar olivine vitrophyre. The 100 kPa (1 atm) liquidus temperature is from that computed by Ref. 1; (B) iron-magnesium partition coefficients between olivine and liquid (see text) at temperatures and pressures indicated (GPa). Dashed lines are from Ref. 2 for low-Ti mare basalt. Ol = olivine [(Mg,Fe)₂SiO₄]; Opx = orthopyroxene [(Fe,Mg)SiO₃]; Grt = garnet [(Ca,Fe,Mg)₃Fe₂Si₃O₁₂]; Liq = liquid.

J. E. Grover, D. H. Lindsley, and A. E. Bence, *Geochim. Cosmochim. Acta, Suppl.*, **14**, 179-196 (1980).

High-pressure and high-temperature experiments were conducted with a synthetic analog of average lunar vitrophyre 14321.¹ Starting materials were oxide mixtures reacted at 920°C at 0.1 MPa in Ag-lined, evacuated silica glass tubes (to form olivine, plagioclase, and clinopyroxene) and run as such, and also with known amounts of forsterite added for reversal experiments. High-pressure experiments were conducted in the solid-media, high-pressure apparatus with Fe containers with a tight-fitting lid. Temperatures were measured with W-Re thermocouples (exact alloy composition is not reported) with no report on thermocouple calibration methods. Temperature probably was uncertain to about $\pm 10^\circ\text{C}$. No pressure calibration was reported either, but most likely is near 0.1-0.2 GPa. Experimental charges were examined with the electron microprobe and with optical microscopy. Detailed analytical results are tabulated in the text.

Pressure-temperature phase relations (A) show olivine on the liquidus to pressures above 2.5 GPa from which observation the authors conclude that olivine vitrophyre is not likely to have been formed by partial melting of the lunar mantle.

Partition coefficients, $K_{\text{Mg}}^{\text{ol-liq}} = X_{\text{MgO}}^{\text{ol}}/X_{\text{MgO}}^{\text{liq}}$, $K_{\text{Fe}}^{\text{ol-liq}} = X_{\text{FeO}}^{\text{ol}}/X_{\text{FeO}}^{\text{liq}}$, and $K_{\text{D}}^{\text{ol-liq}} = X_{\text{FeO}}^{\text{ol}}X_{\text{MgO}}^{\text{liq}}/X_{\text{FeO}}^{\text{liq}}X_{\text{MgO}}^{\text{ol}}$, were calculated from the analytical data (B) and compared with other 0.1 MPa data from Ref. 2 as well as

CaO-FeO-MgO-SiO₂ (concl.)

results from high-pressure experiments.³ Distinct pressure and temperature dependence are noted. Both the $K_{\text{Fe}}^{\text{pl-liq}}$ and $K_{\text{Mg}}^{\text{pl-liq}}$ increased with increasing pressure, whereas K_{D} decreased. These relationships were expressed with the empirical expression in Eq. 1.

$$\ln K_{\text{D}} = aP(\text{GPa}) + 1000b/T(\text{K}) + C \quad (1)$$

The major difference between the present data and those of other published information has been assigned to bulk compositional differences in both liquid and olivine compositions.

The data were used to constrain conditions of formation of high-Mg lunar basalts.

1. F. M. Allen, A. E. Bence, and T. Grove, *Geochim. Cosmochim. Acta, Suppl.*, **11**, 695 (1975).
2. J. Longhi, D. Walker, and J. F. Hays, *Geochim. Cosmochim. Acta*, **42** [10] 1545 (1978).
3. J. F. Bender, F. N. Hodges, and A. E. Bence, *Earth Planet. Sci. Lett.*, **41** [3] 277 (1978).

B.O.M.

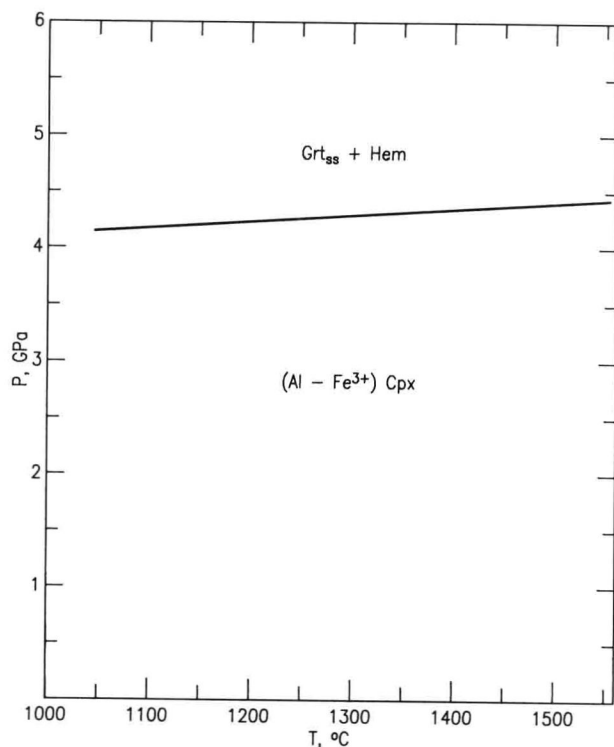
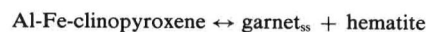
CaO-FeO-Al₂O₃-SiO₂

Fig. 7892—System CaAlFeSiO₆ pyroxene. Pressure-temperature relations at the oxygen fugacity defined by the PtO₂-Pt buffer. Grt_{ss} = garnet solid solution [(Ca,Fe)₃Al₂Si₃O₁₂]; Hem = hematite (Fe₂O₃); Cpx = clinopyroxene (CaAlFeSiO₆).

H. Ohashi and Yu. Hariya, *Gansekai Kobutsu Kosho Gakkaishi*, **70** [3] 93-95 (1975).

High-pressure experiments were conducted in the solid-media, high-pressure, and the belt apparatus with no comments on pressure calibration or uncertainties. Typically, the pressure uncertainties are less than 10% in these types of apparatus. Temperatures were monitored with Pt-Pt87Rh13 thermocouples resulting in $\pm 10^\circ\text{C}$ uncertainty. Starting materials were mechanical mixtures of hematite (Fe₂O₃), wollastonite (CaSiO₃), gehlenite (Ca₂Al₂SiO₇), anorthite (CaAl₂Si₂O₈), and hedenbergite (CaFeSi₂O₆), which were sealed in Pt capsules together with PtO₂ in order to maintain high oxygen fugacity. There is no comment on steps used to eliminate H₂O from the hygroscopic PtO₂. Run durations were from 15 to 40 h, and the experiments were reversed. Although there is no comment on methods of identification, optical and X-ray techniques are commonly used in this type of study, and may have been employed here.

The experimental results for the univariant reaction



show essentially no temperature dependence. The garnet solid solution is on the join grossularite-andradite. Because of the temperature insensitivity, the authors suggest its use as a geobarometer. However, due to the presence of iron, oxygen fugacity also plays an important role that is not considered in the present experiments.

B.O.M.